

KECK OBSERVATORY LASER GUIDE STAR ADAPTIVE OPTICS DISCOVERY AND CHARACTERIZATION OF A SATELLITE TO THE LARGE KUIPER BELT OBJECT 2003 EL₆₁

M. E. BROWN,¹ A. H. BOUCHEZ,^{2,3} D. RABINOWITZ,⁴ R. SARI,¹ C. A. TRUJILLO,⁵ M. VAN DAM,² R. CAMPBELL,²
J. CHIN,² S. HARTMAN,² E. JOHANSSON,² R. LAFON,² D. LE MIGNANT,² P. STOMSKI,² D. SUMMERS,²
AND P. WIZINOWICH²

Received 2005 July 28; accepted 2005 September 2; published 2005 October 3

ABSTRACT

The newly commissioned laser guide star adaptive optics system at Keck Observatory has been used to discover and characterize the orbit of a satellite to the bright Kuiper Belt object 2003 EL₆₁. Observations over a 6 month period show that the satellite has a semimajor axis of $49,500 \pm 400$ km, an orbital period of 49.12 ± 0.03 days, and an eccentricity of 0.050 ± 0.003 . The inferred mass of the system is $(4.2 \pm 0.1) \times 10^{21}$ kg, or $\sim 32\%$ of the mass of Pluto and $28.6\% \pm 0.7\%$ of the mass of the Pluto-Charon system. Mutual occultations occurred in 1999 and will not occur again until 2138. The orbit is fully consistent neither with one tidally evolved from an earlier closer configuration nor with one evolved inward by dynamical friction from an earlier more distant configuration.

Subject headings: comets: general — infrared: solar system — minor planets, asteroids

1. INTRODUCTION

The properties of the orbits of Kuiper Belt object (KBO) satellites hold keys to fundamental insights into the masses and densities of KBOs, the interaction history of the early solar system, the internal structure of distant ice-rock bodies, and the genesis of the Pluto-Charon binary. Progress in characterizing the orbits of KBO satellites has been slow, owing to the fact that observations of closely orbiting satellites have required long-lead-time observations from the *Hubble Space Telescope*, while observations of distant satellites require long baselines to see a full orbital period.

To date, only a small number of relatively small KBO satellites have had their orbits determined (Veillet et al. 2002; Osip et al. 2003; Noll et al. 2004a, 2004b). The total masses of the systems range from 4.2 to 37×10^{18} kg, the orbital eccentricities range from 0.31 to 0.82 , orbital periods range from 46 to almost 900 days, and the flux ratio between the primary and secondary ranges from 1.17 to 1.66 . The Pluto-Charon binary, in contrast, has a mass almost 4000 times higher than the next closest object, an eccentricity close to zero, an orbital period of only 6.4 days, and a flux ratio between Pluto and Charon of about 20 . The great difference in satellite characteristics between the small KBOs and Pluto suggests different mechanisms operating in the different mass regimes.

One of the goals of our ongoing survey for bright KBOs (Trujillo & Brown 2003) is to find higher mass satellite systems that can be used to examine the mass range between these two extremes. The newly discovered KBO 2003 EL₆₁ is one of the brightest known KBOs and thus likely among the most massive. It also has the advantage that it is one of the only currently known KBOs accessible to the newly commissioned laser guide star (LGS) adaptive optics (AO) system at the W. M. Keck

Observatory. Below we describe observations of 2003 EL₆₁ and the discovery and orbital characterization of its satellite with the LGS AO system.

2. OBSERVATIONS

Observations of 2003 EL₆₁ and its satellite were obtained with the LGS AO system (Wizinowich et al. 2005) at the W. M. Keck Observatory using the NIRC2 infrared imager. The LGS AO system works similarly to the natural guide star adaptive optics system (Wizinowich et al. 2000), except that rather than measuring the wave-front aberrations using the light from a natural star, they are determined from observation of laser light resonantly scattered off of sodium atoms in a layer at approximately 90 km altitude in Earth's mesosphere. One limitation of the LGS AO technique is the need to obtain absolute tip-tilt measurement from a natural reference within approximately $1'$ of the target. At the current level of Keck LGS AO performance, this tip-tilt star is required to have $R < 18.5$ mag to achieve nearly diffraction-limited images at $2.1 \mu\text{m}$ (M. van Dam et al. 2005, in preparation). Faint KBOs are difficult to observe for long periods with LGS AO, as appropriate tip-tilt stars are close enough only sporadically. The object 2003 EL₆₁, with a V magnitude of 17.5 (Rabinowitz et al. 2005), is the only known KBO that is bright enough to use as its own tip-tilt source, relieving the difficulties of otherwise highly time-constrained observations.

The observations of 2003 EL₆₁ were performed during six nights of LGS AO commissioning time between 2005 January 26 and June 30, by the Keck Observatory AO engineering team. The object was first acquired by the avalanche photodiode tip-tilt sensor, which kept 2003 EL₆₁ centered in the field by continuously driving the fast tip-tilt mirror. The sodium-dye laser was then projected toward the target, where it was acquired by the fast wave-front sensor. The signal from this fast wave-front sensor was then used to control the 256-actuator deformable mirror to correct for atmospheric aberrations. The laser power output was 12.0 – 13.5 W, creating a reference beacon of equivalent magnitude $11.0 < V < 12.5$ and allowing the high-order loop to be run at 400 Hz. Finally, the focus and high-order image-sharpening control loops were closed between the low-bandwidth wave-front sensor (a separate high-order wave-front

¹ Division of Geological and Planetary Sciences, Mail Code 170-25, California Institute of Technology, 1200 East California Boulevard, Pasadena, CA 91125; mbrown@caltech.edu.

² W. M. Keck Observatory, 65-1120 Mamalahoa Highway, Kamuela, HI 96743.

³ Caltech Optical Observatories, Mail Code 105-24, California Institute of Technology, 1200 East California Boulevard, Pasadena, CA 91125.

⁴ Yale Center for Astronomy and Astrophysics, Yale University, P.O. Box 208121, New Haven, CT 06520.

⁵ Gemini Observatory, 670 North A'ohoku Place, Hilo, HI 96720.

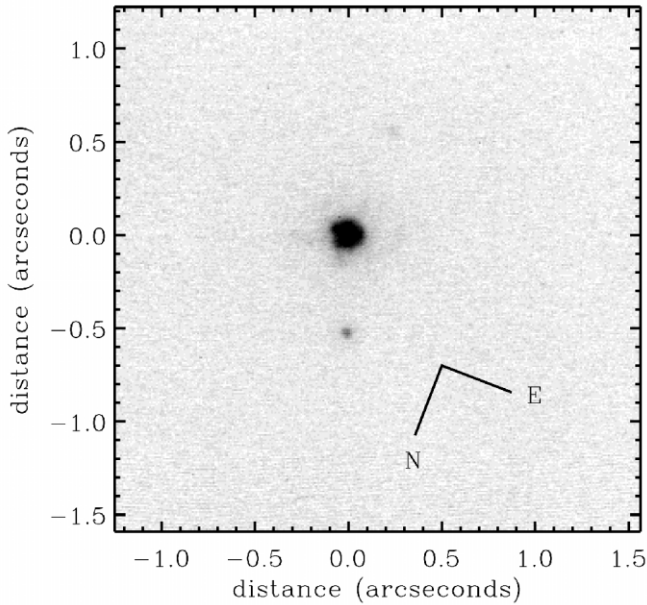


FIG. 1.—Composite LGS AO image of 2003 EL₆₁ and its satellite from the night of 2005 June 30. The faint source directly south of 2003 EL₆₁ is a faint background star, blurred by the motion of 2003 EL₆₁. With the 17.5 mag 2003 EL₆₁ used as a tip-tilt reference, the LGS AO achieved an on-axis Strehl ratio of 0.21 and a FWHM of 62 mas.

sensor observing the tip-tilt reference) and the fast wave-front sensor. This sensor corrects focus offsets due to the variable altitude of the atmospheric sodium layer and quasi-static aberrations caused by the apparent elongation of the laser beacon as seen by the fast wave-front sensor.

While the above acquisition steps were being performed, the NIRC2 imager was configured with a K' filter (1.948–2.299 μm), and $0''.009942 \text{ pixel}^{-1}$ plate scale. Once the LGS AO feedback-loop bandwidths and gains were optimized for the seeing conditions, we recorded several 30 s or 60 s integrations with NIRC2 at each of three dither positions separated by $2''$ – $5''$ on the detector, for a minimum of 360 s total integration.

The images were corrected for sky and instrumental background by subtracting the median of the images in each dither pattern. They were then flat-fielded using twilight-sky flats, and known bad pixels were corrected by interpolation. On one night of attempted observation, poor natural seeing prevented adequate LGS AO correction, but on every other night from the discovery of the satellite on 2005 January 26, the satellite is readily detected in individual 30 or 60 s exposures. Figure 1 shows an image from the most recent night of observation (2005 June 30). Taken under excellent seeing conditions, the June 30 images had a median Strehl ratio of 0.21 and full width at half-maximum of 62 milliarcseconds.

To measure the position of the satellite with respect to the primary, we first fitted the primary with a two-dimensional Gaussian. While a Gaussian is a poor approximation to the actual shape of the image, the center position will still be measured quite accurately. We then fitted the secondary to a two-dimensional Gaussian with the same width as found for the primary. This fitting is performed independently for each individual observation, and the mean and standard deviation of the individual measurements are taken as the offset and measurement error for each night. Table 1 gives a summary of the positions of the satellite over the course of the observations. Any changes in the detector position angle or plate scale over

TABLE 1
SEPARATION OF 2003 EL₆₁ AND ITS SATELLITE

Date (UT)	Mean Time	R.A. Offset (mas)	Decl. Offset (mas)
2005 Jan 26	15:51	35 ± 14	-629 ± 14
2005 Mar 1	12:10	293 ± 23	-1004 ± 23
2005 Mar 4	11:36	339 ± 20	-1263 ± 20
2005 May 27	07:39	-62 ± 10	604 ± 10
2005 Jun 29	07:26	-197 ± 5	520 ± 10

time will contribute to additional error. Long-term monitoring has shown that the position angle is stable to within $0''.2$, and the plate scale to within 0.3% (S. A. Metchev 2005, private communication). Both of these contributions are smaller than the random error.

3. ORBIT FITTING

Fitting the orbit of a solar system satellite requires correctly accounting for the changing viewing geometry due to the motion of Earth and the primary in addition to the orbit of the satellite. With a limited number of observations, the orbital solutions can be plagued by aliases of different orbital periods. Luckily, the spacing of our data rules out spurious aliases. Two of the observations were taken 3 days apart, and the satellite moved $0''.26$ between the two. The solution that we present below forces the motion to be only a fraction of an orbit between these two dates, rather than a full orbit (or more) plus a small fraction. If we were to allow these short-period aliases, the mass of the primary object would have to be at least 10^{25} kg , or about 2 Earth masses, which we reject as unreasonable.

To check for similarity with the Pluto-Charon system, we first attempt to force a circular orbit to the positions of the satellite. The fit uses a Powell χ^2 minimization to find the optimal orbital parameters. For a circular fit, the five parameters are semimajor axis, orbital period, inclination, longitude of the ascending node, and mean anomaly. The best fit finds a semimajor axis of $4.95 \times 10^4 \text{ km}$ and an orbital period of 49.1 days, but it has a χ^2 value of 292, or a reduced χ^2 for 5 degrees of freedom (10 x - y coordinates minus five orbital parameters) of 58. The probability of a χ^2 value this high due to chance is minuscule. We thus reject a circular orbit as a viable solution.

Allowing a full eccentric orbital solution requires adding eccentricity and longitude of perihelion to the orbital parameters. The best eccentric fit is shown in Figure 2 and Table 2 and has a χ^2 value of 0.73, or a reduced χ^2 for 3 degrees of freedom (10 coordinates minus seven orbital parameters) of 0.24. The fit has a marginally lower χ^2 value even than expected, which suggests that we have overestimated the error bars in the positional measurements by approximately a factor of 2. To be conservative, we maintain the current error bars and accept the slightly larger errors. The extremely low value of χ^2 gives us confidence, however, in our previous rejection of the circular orbit and our acceptance of this orbital solution.

Observations of a projected orbit frequently have degeneracies between different solutions that appear identical reflected across the plane of the sky. The changing vantage point of Earth during these observations breaks this degeneracy, however. The difference in predicted positions between the two degenerate solutions differs by more than $0''.05$ across the observing season, well above the measurement uncertainties. The best-fit reflected orbit can be rejected at the more than 99.9% confidence level; thus, we are confident that we have found the single viable orbital solution.

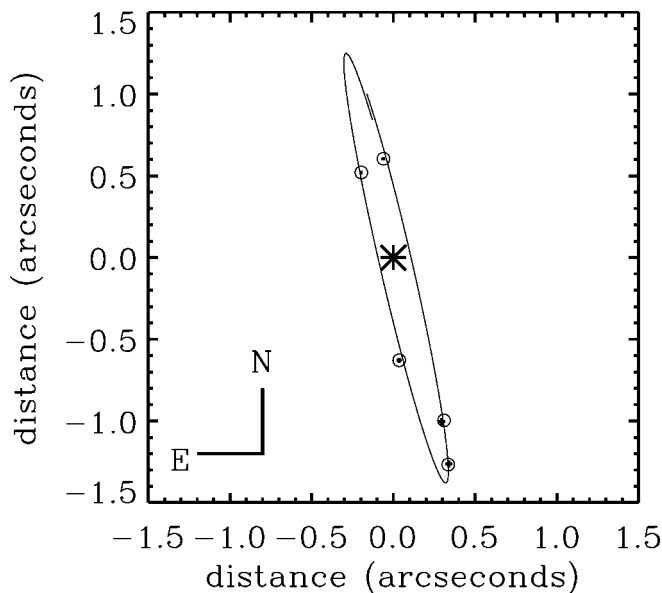


FIG. 2.—Relative position of the satellite compared with 2003 EL₆₁. The very small crosses inside the circles show the LGS AO observations along with their error bars, while the circles show the best-fit orbital solution's predicted locations at the times of the observations. The ellipse shows one full orbit surrounding the mean date of the observations. The slight discrepancies between this projected orbit and the positions of the predictions is caused by the changing Earth–2003 EL₆₁ viewing geometry across the 6 months of observation.

We determine errors in the individual parameters through Monte Carlo simulation. We perform 1000 iterations of orbit optimization where we add Gaussian noise with σ equal to the measurement errors of the position measurements and solve for new orbital parameters. We define the 1σ error bars on the parameters to be the range containing the central 68% of the data. Table 2 gives the ecliptic orbital elements of the satellite orbit.

The uncertainties on the individual orbital parameters are not independent, and thus uncertainties on quantities obtained from multiple parameters need to be determined separately through Monte Carlo analysis. The mass, in particular, depends on both semimajor axis and period. We calculate the retrieved mass independently in each Monte Carlo simulation and define the uncertainty in the final mass identically to the manner for the individual parameters above. The final retrieved mass of the 2003 EL₆₁–plus–satellite system is $(4.2 \pm 0.1) \times 10^{21}$ kg, or $\sim 32\%$ of the mass of Pluto and $28.6\% \pm 0.7\%$ of the mass of the Pluto–Charon system. From relative photometry on 2005 June 30, the satellite is 3.3 mag fainter than the primary, so for a similar density and albedo, it contributes only 1% of the mass and can thus be neglected.

One method of obtaining detailed information on the shapes of the objects in such a system is through observations of mutual eclipses, analogous to those observed for Pluto and Charon in the 1980s (Binzel & Hubbard 1997). The satellite system is currently only 4° from being viewed edge-on. Unfortunately, the system is moving away from its edge-on configuration. The orbit was last edge-on in late 1999 and will not be again for 133 years, in 2138.

4. DISCUSSION

The 2003 EL₆₁ system contains more than 1000 times the mass of the next most massive measured Kuiper Belt satellite

TABLE 2
ORBITAL PARAMETERS

Parameter	Value
Semimajor axis	$49,500 \pm 400$ km
Inclination	$234^\circ 8 \pm 0^\circ 3$
Period	49.13 ± 0.03 days
Eccentricity	0.050 ± 0.003
Argument of perihelion	$278^\circ 6 \pm 0^\circ 4$
Longitude of ascending node	$26^\circ 1 \pm 0^\circ 4$
Time of pericenter passage	JD 2,453,458.40 \pm 0.02

NOTE.—Relative to J2000 ecliptic.

system and is within a factor of 4 of the mass of the Pluto–Charon system. The 0.050 eccentricity of the satellite is much closer in character to the circular orbit of the Pluto–Charon system than the higher eccentricities of the other systems. One significant difference between the 2003 EL₆₁ system and the Pluto–Charon system, however, is that while Pluto and Charon are locked into 6.3 day rotation periods commensurate with their 6.3 day orbit, 2003 EL₆₁ has a high-amplitude double-peaked 3.9 hr rotation period, which is significantly shorter than the 49.1 day orbital period of the satellite (Rabinowitz et al. 2005). For all physically possible values of its density, 2003 EL₆₁'s spin angular momentum dominates by orders of magnitude the orbital angular momentum of the system. The object's spin is slowed little by its satellite, owing to the likely very small relative mass of the satellite.

The fast spin of the primary and the near-circular orbit of the satellite suggest formation by impact. Detailed simulations of the higher mass Pluto–Charon–forming impacts show that satellites with a few percent of the mass of the primary can be formed in many different types of collisions (Canup 2005). If such a collision occurs, the satellite orbit then must tidally evolve to its present position. We can estimate the expected orbital period of the satellite after 4.5 Gyr of evolution as

$$P = (58 \text{ days}) \left(\frac{k/1.5}{Q/100} 90q \right)^{3/13} \left(\frac{\rho}{1 \text{ g cm}^{-3}} \right)^{-5/13}, \quad (1)$$

where k is the tidal Love number, q is the ratio of the satellite's to the primary's mass, and ρ is the density of the primary. For a purely fluid body with $k = 1.5$, this 58 day estimate is in reasonably good agreement with the observed 49 day orbital period, but for any reasonable value of strength the period drops well below that observed.

Tidal evolution will affect the eccentricity as well as the period. The amount and direction of eccentricity evolution depends on the strengths of 2003 EL₆₁ and the satellite. If 2003 EL₆₁ is strengthless while the satellite is not, eccentricity evolves mostly as a result of tides on 2003 EL₆₁, which cause eccentricity to increase on the same timescale as the semimajor-axis increase. Such an increasing eccentricity is inconsistent with the low eccentricity of the satellite orbit. If both bodies are strengthless, then tides on the satellite dominate the eccentricity evolution and cause it to damp. The timescale for eccentricity damping can be estimated as

$$\left| \frac{\dot{e}/e}{\dot{a}/a} \right| = \frac{7}{2} \left(\frac{m_p}{m_s} \right) \left(\frac{r_s}{r_p} \right)^5 \left(\frac{k_s}{k_p} \right) \left(\frac{Q_p}{Q_s} \right) = \frac{7}{2} \left(\frac{r_p}{r_s} \right), \quad (2)$$

where the second equality assumes that both bodies have similar quality factors and similar densities. The eccentricity-damping timescale is about 15 times shorter than the orbital

evolution timescale, which is by assumption the age of the system. Therefore, the eccentricity of the satellite damps every 300 Myr and should be expected to be extremely small. The 0.05 eccentricity of the system thus appears difficult to explain from orbital evolution alone. Stern et al. (2003) considered perturbations from surrounding bodies as a method to excite the putative eccentricity of the Pluto-Charon system. Scaling their detailed calculations to the circumstances of 2003 EL₆₁, we find that typical eccentricities for the 2003 EL₆₁ system should be on the order of $e \approx 0.003$, much smaller than the observed eccentricity. While a recent strong perturbation cannot be ruled out, the probability of such an event is extremely low.

An alternative to tidal evolution of the system is that the system formed by capture and the semimajor axis was decreased by dynamical friction (Goldreich et al. 2002). While bodies of equal mass can evolve to become contact binaries, bodies of unequal mass evolve to have a semimajor axis of approximately the primary radius times the mass ratio. The estimated period is approximately a factor of 3 higher than that measured here, but the estimate is likely good only to an order

of magnitude and so may be consistent. It is unknown how the eccentricity should evolve in this case. Given our current understanding of the outer solar system, neither formation scenario is entirely satisfying for explaining both the moderate orbital period and small but significant eccentricity of the system.

This research is supported by a Presidential Early Career Award from the NASA Planetary Astronomy Program. Data presented herein were obtained at the W. M. Keck Observatory, which is operated as a scientific partnership among the California Institute of Technology, the University of California, and the National Aeronautics and Space Administration. The observatory was made possible by the generous financial support of the W. M. Keck Foundation. The authors wish to recognize and acknowledge the very significant cultural role and reverence that the summit of Mauna Kea has always had within the indigenous Hawaiian community. We are most fortunate to have the opportunity to conduct observations from this mountain.

REFERENCES

- Binzel, R. P., & Hubbard, W. B. 1997, in *Pluto and Charon*, ed. S. A. Stern & D. J. Tholen (Tucson: Univ. Arizona Press), 85
- Canup, R. M. 2005, *Science*, 307, 546
- Goldreich, P., Lithwick, Y., & Sari, R. 2002, *Nature*, 420, 643
- Noll, K. S., Stephens, D. C., Grundy, W. M., & Griffin, I. 2004a, *Icarus*, 172, 402
- Noll, K. S., Stephens, D. C., Grundy, W. M., Osip, D. J., & Griffin, I. 2004b, *AJ*, 128, 2547
- Osip, D. J., Kern, S. D., & Elliot, J. L. 2003, *Earth Moon Planets*, 92, 409
- Rabinowitz, D. L., Barkume, K., Brown, M. E., Schwartz, M., Tourtellotte, S., & Trujillo, C. 2005, *ApJ*, submitted (astro-ph/0509401)
- Stern, S. A., Bottke, W. F., & Levison, H. F. 2003, *AJ*, 125, 902
- Trujillo, C. A., & Brown, M. E. 2003, *Earth Moon Planets*, 92, 99
- Veillet, C., et al. 2002, *Nature*, 416, 711
- Wizinowich, P., et al. 2000, *PASP*, 112, 315
- . 2005, *PASP*, submitted